Available online at www.sciencedirect.com
ScienceDirect
Neurocomputing 70 (2007) 1970–1976
NEUROCOMPUTING
www.elsevier.com/locate/neucom

Coherence resonance due to correlated noise in neuronal models

Thomas Kreuz[a,*], Stefano Luccioli[a,b], Alessandro Torcini[a]

[a]*Istituto dei Sistemi Complessi - CNR, via Madonna del Piano 10, Sesto Fiorentino I-50019, Italy*
[b]*INFN, Dipartimento di Fisica, Universitá di Firenze, via Sansone, Sesto Fiorentino, 1 - I-50019, Italy*

Available online 15 November 2006

Abstract

We study the regularity of noise-induced excitations in the FitzHugh–Nagumo (FHN) neuronal model subject to excitatory and inhibitory high-frequency input with and without correlations. For each value of the correlation a relative maximum of spike coherence can be observed for intermediate noise strengths (coherence resonance). Moreover, the FHN system exhibits an absolute maximum of coherent spiking for intermediate values of both the noise amplitude and the strength of correlation (double coherence resonance). The underlying mechanisms can be explained by means of the discrete input statistics.

Keywords: Single neuron model; FitzHugh–Nagumo; Coherence resonance; Noise; Correlations

1. Introduction

Neuronal models are among the most widely used dynamics to study the phenomenology of excitable systems under the influence of noise. Apart from the much simpler integrate-and-fire (IF) model the four-dimensional Hodgkin–Huxley (HH) [6] and its reduction to two dimensions, the FitzHugh–Nagumo (FHN) model [4], constitutes the most common models in theoretical neuroscience. Both models consist of differential equations that are able to reproduce observed neuronal behavior such as excitability and refractoriness. When these models are driven by noise, a variety of excitation phenomena including stochastic resonance and coherence resonance has been observed (for an overview please refer to [10]). Whereas *stochastic resonance* [5] refers to an enhanced detectability of weak (subthreshold) periodic signals for an intermediate amount of noise, *coherence resonance* [12] describes the occurrence of an increased regularity of the response driven by an appropriately chosen amount of noise, in this case no external signal is needed. This effect has been observed for a great variety of neuronal models such as HH [9,11] and FHN [12].

In excitable systems the classical coherence resonance with respect to the noise strength can be explained by the different dependencies of slow activation and fast excitation on the noise strength [12,13]. The occurrence of a minimum in the coefficient of variation (the standard deviation of the distribution of interspike intervals (ISI) normalized by its mean) for noise levels in between these extremes is considered as a key indication for coherence resonance. By using colored noise instead of white-noise coherence resonance with respect to the correlation length has also been observed [1]. In the context of neuronal dynamics continuous noise is often replaced by discrete noise kicks reflecting the synaptic input received from excitatory and inhibitory presynaptic neurons. Theoretical studies using such correlated input comprise [3,14,15,17]. A comprehensive analysis giving an explanation for coherence resonance with respect to the correlation in such an environment is still missing and thus declared the aim of the present study.

2. Model and methods

The FHN model [4] is a two-dimensional reduction of the HH model with a voltage-like variable V and a recovery-like variable W:

$$\frac{dV}{dt} = \phi\left(V - \frac{V^3}{3} - W\right),$$

*Corresponding author. Tel.: +39 055 5226626; fax: +39 055 5226683.
E-mail address: thomas.kreuz@fi.isc.cnr.it (T. Kreuz).

0925-2312/$ - see front matter © 2006 Elsevier B.V. All rights reserved.
doi:10.1016/j.neucom.2006.10.129

$$\frac{dW}{dt} = V + a + I_0 - I(t). \quad (1)$$

The time-scale separation is set to $\phi = 100$ and the bifurcation parameter is chosen to be $a = 1.05$. For this parameter, the dynamics is in the vicinity of a supercritical Hopf bifurcation (cf. [12]) with only one attractor, a stable focus fixed point at $V = 1.05$ and $W = -0.664$. If a silent FHN neuron is forced by just one kick of sufficient strength it emits a spike and relaxes to its fixed point via a damped oscillation. Here, we use a much smaller kick amplitude of $\Delta W = 0.0014$ and kick rates of $r = 0.3$. The dynamics is integrated by employing a fourth-order Runge–Kutta scheme with a step size of $\delta t = 10^{-4}$. A spike is identified whenever $V(t)$ overcomes a fixed detection threshold $\Theta = 0.4$.

The presynaptic input is modeled as the superposition of N_e excitatory and N_i inhibitory trains of post-synaptic potentials (PSPs)

$$I(t) = \Delta W \left[\sum_{k=1}^{N_e} \sum_{l} \delta(t - t_k^l) - \sum_{m=1}^{N_i} \sum_{n} \delta(t - t_m^n) \right], \quad (2)$$

where t_k^l and t_m^n are the respective arrival times of the instantaneous voltage kicks of strength ΔW. Since the single-neuron model does not distinguish the origin of its input, it is sufficient to generate only two over-all kick trains (one excitatory and one inhibitory) with the given dependencies and given over-all rates R_e and R_i. Each of the two kick trains is considered to be the overlap of N_e excitatory and N_i inhibitory kick trains following a Poissonian distribution with individual rates $r_e = R_e/N_e$ and $r_i = R_i/N_i$. Correlated kick trains are generated by using a refined method based on the idea of shared input (cf. [14,15,17]). The average fraction of shared kicks between any two individual trains is given by the three pair-wise correlation coefficients: excitatory–excitatory C_{ee}, inhibitory–inhibitory C_{ii} and excitatory–inhibitory C_{ei}.

In this study, we restrict ourselves to cases with one type of correlations only (i.e., C_{ei} and either C_{ee} or C_{ii} are set to zero). Thus, the two kick trains can be created separately: the uncorrelated kick train is generated from a Poissonian distribution with the desired rate R_x (where x can stand for excitatory or inhibitory). The kick train with correlations $C_{xx} > 0$) is obtained from a Poissonian distribution with the desired rate R_x, and the amplitudes w of the single kicks are successively drawn from the binomial distribution with the probability $p = C_{xx}$ and the total number of neurons $n = N_x$:

$$p_w^{(N_x)} = \frac{N_x!}{w!(N_x - w)!} C_{xx}^w (1 - C_{xx})^{N_x - w}. \quad (3)$$

The average strength of excitatory and inhibitory kicks (in units of ΔW) is thus given by the expectation value of the binomial distribution $W_e = C_{ee} * N_e$ and $W_i = C_{ii} * N_i$. Note that by using this procedure the C_{xx} are, apart from statistical fluctuations, identical to the Pearson correlation coefficients obtained for the average net spike counts of pairs of neurons (cf. [15]).

The mean current $\bar{I} = C\Delta W r(N_e - N_i)$ is proportional to the average net count $\mu = (N_e - N_i)\Delta T r$ within a temporal window. Since in our simulations we always set $r_e = r_i \equiv r$ and $N_e = N_i \equiv N$ we have a balanced synaptic input. Thus, the neuron is driven by fluctuations and not by a drift towards threshold, a condition that renders the neuron more sensitive to input correlations [15]. By varying the number of presynaptic neurons N, we can control both the variance of the net count $Q^2 = \Delta T r(N_e + N_i)$ and the variance of the current. In agreement with [3,15] the latter is proportional to $\sigma = r(\Delta W)^2(C_{ee}N_e^2 + (1 - C_{ee})N_e + C_{ii}N_i^2 + (1 - C_{ii})N_i)$. Thus the properties of the input are completely determined by the variance and the correlation. An increase of the variance is equivalent to an increase of the number of neurons. For uncorrelated noise this leads to an increase of the kick frequency while for fixed positive correlation it causes an increase of the kick amplitude (whereas the frequency of the correlated kicks remains constant). For constant variance the kick amplitude increases and the kick frequency decreases with the correlation. Due to the influence of the number of neurons, the frequency of the uncorrelated kicks also decreases with increasing correlation.

In the following, we characterize the coherence in the neuronal response in dependence on both of these parameters. The variance is increased equidistantly on a logarithmic scale, while the correlation is changed in steps of 0.1 from full-excitatory correlation to full-inhibitory correlation (including the intermediate case of no correlation at all). As an indicator of coherence resonance we employ the coefficient of variation $C_V = \sqrt{\mathrm{var}(t_{ISI})}/\langle t_{ISI} \rangle$ from the distribution of ISIs t_{ISI}. This quantity attains the value 0 for a perfectly periodic response and the value 1 for Poissonian output. Similar results have been obtained with the correlation time τ_c of the ISI time series and with conditional entropies.

3. Results

The C_V of the neuronal response exhibits a minimum for intermediate values of the variance for the whole range of correlations (cf. Fig. 1). But not only the value and the position of this minimum are shifted for different correlations, also the underlying mechanisms are completely different, as we will show in the following starting with the extreme case of full correlation. For this case we can assume that the uncorrelated input constitutes a quasi-continuous background since the correlated kicks are emitted with a lower rate (which for fixed correlation is independent of the variance) but higher amplitude (which increases with the variance).

For the case of full correlation in the excitatory input the ISI-distribution remains Poissonian for all variances (cf. Fig. 2), although the course of the C_V has a z-like shape. For low variance we have an activation process

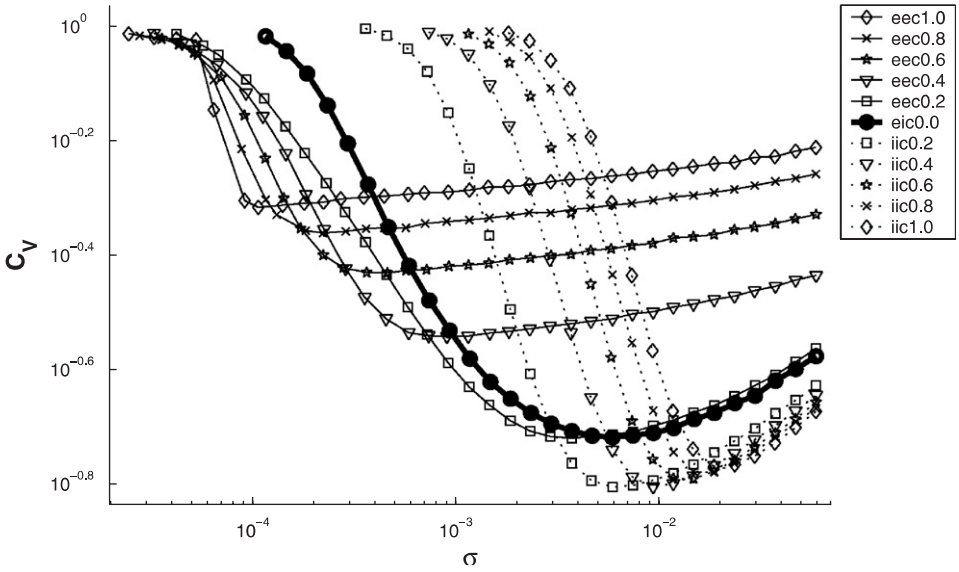

Fig. 1. Coefficient of variation C_V versus variance for different values of the correlation coefficients: only excitatory (eec#, solid lines), only inhibitory (iic#, dotted lines) or no correlation at all (eic0.0, thick line).

following Kramer's law and since the mean ISI-interval $\langle t_{ISI}\rangle$ is much larger than the refractory time t_{ref}, the C_V is according to $C_V^{Poisson} = 1 - t_{ref}/\langle t_{ISI}\rangle$ close to 1 (Fig. 2a). With increasing variance (i.e., increasing amplitude of the kicks) we observe a sudden decrease of the C_V at the amplitude for which one kick can be enough to trigger a spike (depending on the voltage at the time of the kick). This decrease comes to an end and we have a minimum of the C_V (Fig. 2b) at the variance for which in principle each kick is sufficient to cross the seperatrix which acts as a threshold in the state space of the FHN model (cf. [8]). From then on, the Poissonian shape follows from an almost 1:1 synchronization between excitatory kicks and spikes. The increase of the C_V with the variance is due to the fact that the still increasing amplitudes lead to a decrease of the refractory time (Fig. 2c).

The same mechanism is active in the case of lower correlation in the excitation with the only difference that the minimum of the C_V is shifted to lower values and higher variances (cf. right parts of Fig. 3 and its inset). The shift to lower values occurs since for lower correlation the frequency of the spike-provoking kicks is higher leading to a lower t_{ISI} and thus also to a lower C_V while the shift to higher variances is due to the decrease of the average kick amplitude with decreasing correlation. Still the minimum is attained when the whole distribution of kick amplitudes has crossed the threshold, however, now the transition to 1:1 synchronization is more smooth since the kick amplitudes now follow a binomial distribution so that the variance region for which only a part of the kicks suffices to trigger a spike gets broader. In this manner for increasing variances the minimum is obtained for smaller and smaller correlations (cf. Fig. 1) such that for a fixed variance we observe a minimum of the C_V for an intermediate value of the correlation. This is coherence resonance with respect to the correlation length. During this shift of the transition point to higher variances (cf. inset of Fig. 3) the frequency of the uncorrelated inhibitory kicks increases more and more (the quasi-continuous inhibitory background current gets stronger effectively shifting the bifurcation parameter a to higher values) so that for a certain excitatory correlation even at high variances one kick is rarely enough to trigger a spike. Thus at this correlation we observe a dip in Fig. 3. This point satisfies three conditions: the amplitudes of correlated excitatory kick are high enough to reach 1:1 synchronization, the frequency of the correlated excitatory kicks is so low that the Poissonian tail almost disappears and, finally, the variance of the minimum and thus the frequency of inhibitory kicks are so low that they allow 1:1 synchronization.

A completely different mechanism is responsible for the case of full correlation in the inhibitory input (cf. Fig. 4). Spiking sets in at quite high variances only when the rate of the uncorrelated excitatory kicks (which form the underlying current driving the neurons towards threshold) has become high enough to recover from the last inhibitory kick and to reach the spiking threshold before the next inhibitory kick. Resembling an activation process the ISI distribution is Poissonian with a C_V close to 1 (Fig. 4a). For higher variances the increasing excitatory background renders the mean ISI shorter and shorter (and so the value of the C_V gets smaller) until a regime of almost repetitive firing is reached (Fig. 4b). Finally the increasing amplitude of the inhibitory kicks leads to a quantization reflected by a multi-modality in the ISI histogram and a corresponding increase in the C_V (Fig. 4c).

This quantization is due to the fact that each inhibitory kick (except the ones in the refractory time) disturbs the repetitive firing, delays the next spike and thus prolongs the

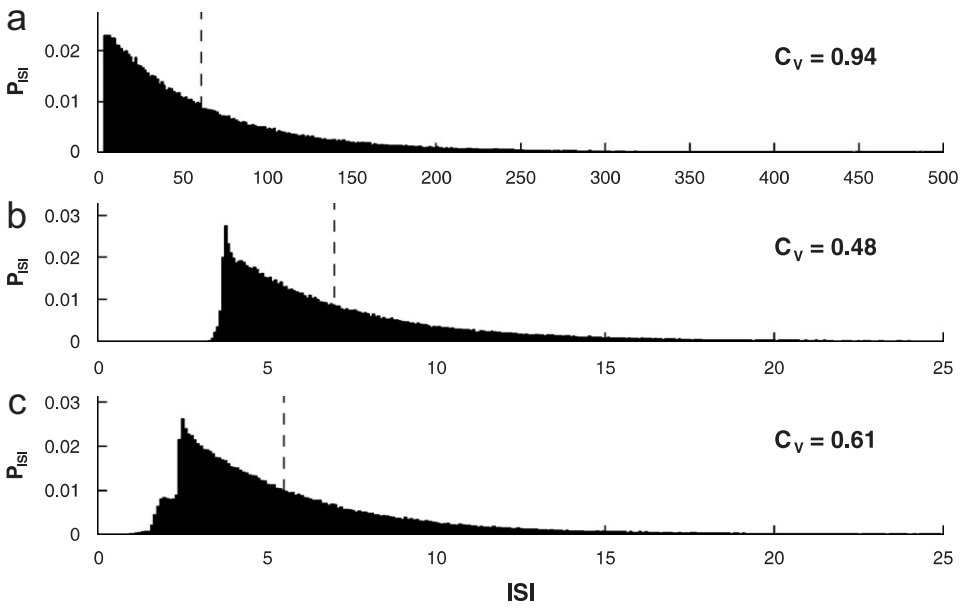

Fig. 2. Full excitatory correlation: ISI-histogram for three different variances. (a) Low variance: activation process, (b) intermediate variance (minimum of C_V): 1:1 synchronization with high refractory time, (c) high variance: 1:1 synchronization with reduced refractory time. Dashed lines mark the mean ISI. Please note the different x-scale for the first histogram.

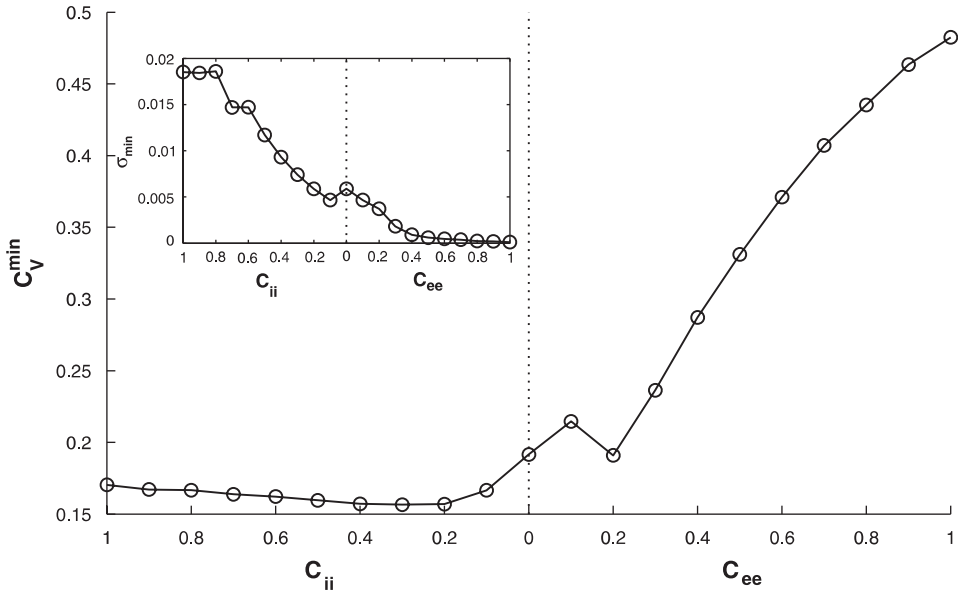

Fig. 3. Minimum value of the C_V versus correlation. Inset: variance at which the minimum value of the C_V is obtained versus correlation.

ISI (the quasi-continuous excitatory background first has to recover the last inhibitory kick before it can continue to drive the neuron towards threshold). The ISI-histogram can be regarded as a superposition of many peaks (each peak corresponding to a fixed number of kicks per spikes K) which generally overlap substantially as can be seen from the vertical projections of the point clouds in the inset of Fig. 5. Only for high variances and correlations the quantization is so high that the importance of the number of kicks overshadows the importance of their position (i.e., the distance between the center of masses of different clouds becomes higher than the horizontal spreading in each cloud). This leads to the multi-peak ISI-histogram observed in Fig. 4c.

From the proportionality between the ISI-length and the number of inhibitory kicks, the average delay per inhibitory kick $\langle D\rangle$ can be estimated (cf. Fig. 5, inset). This quantity, together with the number of inhibitory kicks per spike K, is sufficient to yield a remarkably exact estimate of the course of the C_V (cf. Fig. 1):

$$C_V = \sqrt{var(t_{ISI})}/\langle t_{ISI}\rangle \approx \frac{\langle D\rangle \Delta K + \Delta D \langle K\rangle}{t_{rp} + \langle D\rangle\langle K\rangle}, \tag{4}$$

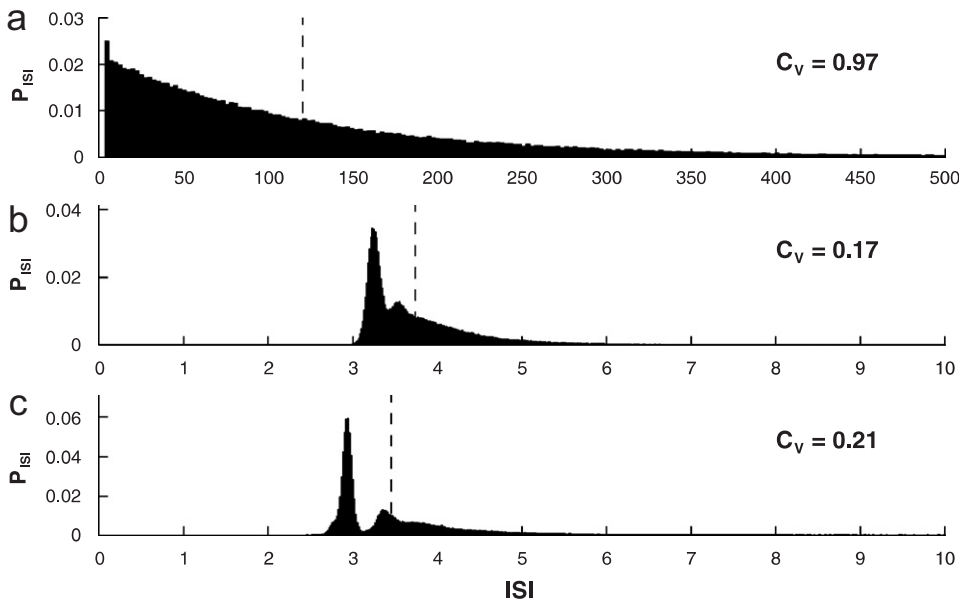

Fig. 4. Full inhibitory correlation: ISI-histogram for three different variances. (a) Low variance: activation process, (b) intermediate variance (minimum of C_V): repetitive firing with only small quantization, (c) high variance: repetitive firing with multiple peaks due to quantization. Dashed lines mark the mean ISI. Please note the different x-scale for the first histogram.

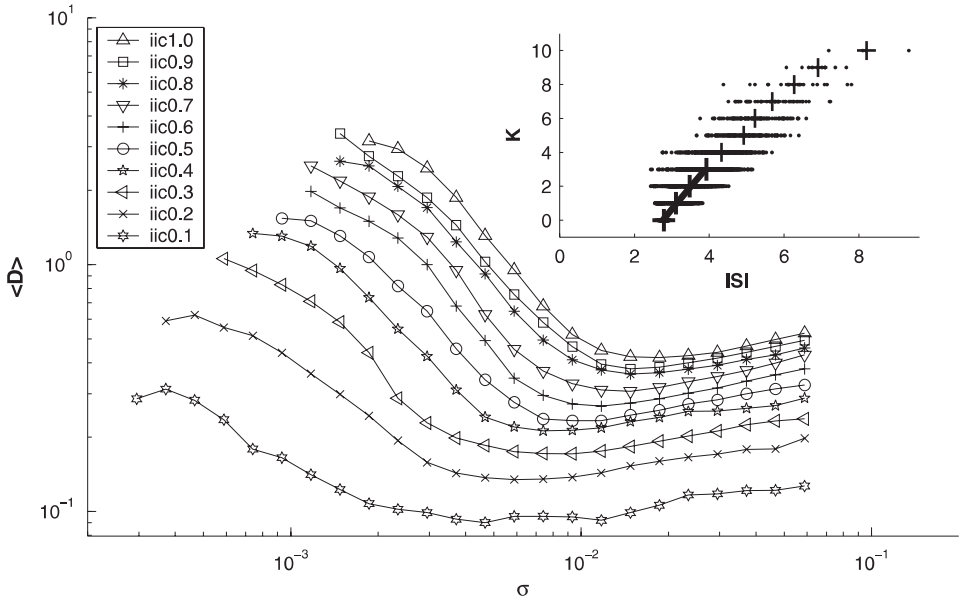

Fig. 5. Average delay per inhibitory kick $\langle D\rangle$ versus variance for different values of inhibitory correlation. Inset: exemplary scatter plot of the number of kicks K in a given ISI versus the length of the respective ISI (inhibitory correlation $C_{ii} = 0.6$ and maximum noise strength $\sigma = 0.06$, data obtained from 6000 ISIs). Black crosses mark the center of mass for each number of kicks; thick black crosses highlight the ones with the highest statistics (i.e., those inside the main peak of the ISI histogram) that are used to estimate the average delay per kick $\langle D\rangle$ as the inverse of the derivative of the linear fit.

with t_{rp} being the ISI expected for repetitive firing without inhibitory disturbance (i.e., the point where the fit in the inset of Fig. 5 crosses the x-axis). Only for high variances the estimate is too a little too low since there the standard deviation within each of the multiple peaks should be taken into account as well. In this estimate the coherence resonance is reflected by the minima of the average delay per inhibitory kick $\langle D\rangle$ for each correlation (cf. Fig. 5).

Comparing different correlations, for the highest variances the minimum of the C_V is obtained for the full inhibitory correlation (cf. Fig. 1). Although here the quantization is by far more pronounced, the higher

amplitude is less effective in disturbing than the high frequency since for the latter there are more kicks in the small time window between the end of the refractory time and the next spike. For decreasing inhibitory correlation, the repetitive firing state is reached already for lower variances since the rate of the uncorrelated excitatory kicks increases with decreasing correlation. Also the minimum of the C_V decreases since for lower correlation (in particular at lower variances) we have lower amplitudes of the correlated kicks and thus less quantization. For the lowest correlation we do not even reach the state of repetitive firing (and thus the C_V does not reach very low values) since the frequency of the correlated kicks is so high that it disturbs significantly even in the short interval between the end of the refractory time and the beginning of the spike (for lowest correlation the average frequency ratio between the uncorrelated excitatory and the correlated inhibitory kicks is minimal).

Since for all correlations the minimum of the C_V is attained for intermediate values of the variance we have coherence resonance with respect to the noise strength. Except for some very low and for the highest variances the minimum is also obtained for an intermediate value of the correlation, thus we observe coherence resonance with respect to the correlation length. Furthermore, since the overall absolute minimum is obtained for intermediate values of both the noise strength and the correlation, we have a double coherence resonance (DCR). Also this prominent point satisfies three conditions: the frequency of the excitatory background is high enough to allow repetitive firing, whereas both the frequency and the amplitude of the correlated inhibitory kicks are low enough not to disturb (quantize) too much (the trade-off between the frequency and the amplitude is optimal).

The results shown here have been obtained for an input rate $r = 0.3$. Results for different rates can be related to these values by a parameter transformation. The important parameter is not the correlation C_{xx} but $\langle T\rangle = C_{xx}/r = C_{xx}\langle t\rangle$, the average interval between the correlated kicks (with t being the average interval between the uncorrelated kicks). For cases with identical $\langle T\rangle$ also the average amplitude $\mu = NC_{xx}$ of correlated kicks is independent of the rate, however, the standard deviation $\sigma = \sqrt{NC_{xx}(1 - C_{xx})}$ of the binomial amplitude distribution is lower for the case in which both correlation and rate are lower. For correlated inhibitory kicks this does not make a difference but for correlations in the excitatory input the crossing of the spike triggering threshold is affected. The dip is most pronounced for the case of highest correlation and highest rate since there the complete 1:1 synchronization is already reached at the lower variances where the refractory time and also the mean are still rather large and thus the C_V is still quite low.

4. Conclusion

By means of a new discrete method to generate correlated pre-synaptic input we could explain the double coherence resonances in the FitzHugh–Nagumo model. Starting from the two extreme cases of full correlation in excitation and inhibition we could disclose the different mechanisms responsible for the minimum in the C_V: for fixed excitatory correlation the occurrence of the minimum is a pure kick amplitude effect whereas the decrease of the minimum C_V with decreasing correlation is due to the change in the frequency of the correlated kicks. The increase for very low correlations is an effect of the change in the frequency of the uncorrelated kicks. Different dependencies are observed for fixed inhibitory correlation where the occurrence of the minimum in the C_V is a combined effect of the uncorrelated excitatory frequency and the correlated inhibitory kick amplitude. The decrease of the minimum C_V with decreasing correlation is due to the change in the frequency of the correlated kicks whereas the increase for very low correlations is an effect of the change in the frequency of the uncorrelated kicks. The uncorrelated case marks the smooth transition from one kind of correlation to the other and can thus be understood as the lower limit case for both kinds of correlated inputs.

We believe that the present results can be useful to gain some deeper understanding on the role of correlations in neuronal coding [7,16]. Future work will include the application of this and more complicated correlation schemes (e.g., schemes including cross-correlations between excitation and inhibition) to more realistic neuronal models in order to simulate the role of correlations in the high-conductance state of neocortical neurons in vivo [2]. Another promising direction of research could be the analysis of correlation effects on synchronization properties of neuronal networks.

Acknowledgement

We acknowledge useful discussions with A. Politi. T.K. has been supported by the Marie Curie Individual Intra-European Fellowship "DEAN", Project No. 011434.

References

[1] J.M. Casado, Noise-induced coherence in an excitable system, Phys. Lett. A 235 (1997) 489.
[2] A. Destexhe, M. Rudolph, D. Paré, The high-conductance state of neocortical neurons *in vivo*, Nat. Rev. Neurosci. 4 (2003) 739.
[3] J. Feng, P. Zhang, Behavior of integrate-and-fire and Hodgkin–Huxley models with correlated inputs, Phys. Rev. E 63 (2001) 051902.
[4] R. FitzHugh, Impulses and physiological states in theoretical models of nerve membrane, Biophys. J. 1 (1961) 445.
[5] L. Gammaitoni, P. Haenggi, P. Jung, F. Marchesoni, Stochastic resonance, Rev. Mod. Phys. 70 (1998) 223.
[6] A.L. Hodgkin, A.F. Huxley, A qualitative description of membrane current and its application to conduction and excitation in nerve, J. Physiol. (London) 117 (1952) 500.
[7] A.V. Holden, Neural coding by correlation, Nature 428 (2004) 382.
[8] C. Koch, Biophysics of Computation, Oxford University Press, New York, 1999.
[9] S.G. Lee, A. Neiman, S. Kim, Coherence resonance in a Hodgkin–-Huxley neuron, Phys. Rev. E 57 (1998) 3292.

[10] B. Lindner, J. Garcìa Ojalvo, A. Neiman, L. Schimansky-Geier, Effects of noise in excitable systems, Phys. Rep. 392 (2004) 321.
[11] S. Luccioli, T. Kreuz, A. Torcini, Dynamical response of the Hodgkin–Huxley model in the high-input regime, Phys. Rev. E 73 (2006) 041902.
[12] A.S. Pikovsky, J. Kurths, Coherence resonance in a noised-driven excitable system, Phys. Rev. Lett. 78 (1997) 775.
[13] J.R. Pradines, G.V. Osipov, J.J. Collins, Coherence resonance in excitable and oscillatory systems: the essential role of slow and fast dynamics, Phys. Rev. E 60 (1999) 6407.
[14] M. Rudolph, A. Destexhe, Correlation detection and resonance in neural systems with distributed sources, Phys. Rev. Lett. 86 (2001) 3662.
[15] E. Salinas, T.J. Sejnowski, Impact of correlated synaptic input on output firing rate and variability in simple neuronal models, J. Neurosci. 20 (2000) 6193.
[16] E. Salinas, T.J. Sejnowski, Correlated neuronal activity and the flow of neural information, Nat. Rev. Neurosci. 2 (2001) 539.
[17] M.N. Shadlen, W.T. Newsome, The variable discharge of cortical neurons: implications for connectivity, computation and information coding, J. Neurosci. 18 (1998) 3870.

Thomas Kreuz is Marie Curie fellow at the Institute of Complex Systems (ISC) in Florence, Italy (Head: Dr. Politi). Before he has done computational neuroscience research at the Department of Epilepsy in Bonn, Germany (Head: Prof. Elger) and at the John von Neumann Institute of Computing (NIC) at the research center Juelich, Germany (Head: Prof. Grassberger) where he obtained his Ph.D. in physics in 2003. His research expertise includes nonlinear time series analysis, synchronization, nonlinear dynamics, and epileptic seizure prediction. His current work deals with simulations of neuronal models under the influence of noise combined with the analysis of single neuron recordings.

Stefano Luccioli obtained his MS (Laurea) in Physics at the University of Florence (Italy) in 2005. He is presently receiving his Ph.D. training in nonlinear dynamics and complex systems at the University of Florence. His Ph.D. thesis deals with mechanically induced folding and unfolding of heteropolymers.

Alessandro Torcini obtained his M.S. (Laurea) and Ph.D. in Theoretical Physics at the University of Florence (Italy). He received postdoctoral training at Wuppertal (Germany), Marseille (France), Florence and Rome (Italy). He pursues his research activity at the Institute of Complex Systems (CNR) in Florence on the following subjects: nonlinear dynamics of complex systems and analyses of statistical and dynamical properties of biologically inspired models of polymers and neuronal systems.